SynBio

MDPI

Article

Analysis and Application of Translation-Enhancing Peptides for Improved Production of Proteins Containing Polyproline

Akimichi Yoshino [1], Riko Shimoji [2], Yuma Nishikawa [2], Hideo Nakano [2] and Teruyo Ojima-Kato [2,*]

[1] Laboratory of Molecular Biotechnology, Faculty of Agriculture, Nagoya University, Furo-cho, Chikusa-ku, Nagoya 464-8601, Japan; yoshino.akimichi@molbiotech-nagoya.org
[2] Laboratory of Molecular Biotechnology, Graduate School of Bioagricultural Sciences, Nagoya University, Furo-cho, Chikusa-ku, Nagoya 464-8601, Japan; shimoji.riko@molbiotech-nagoya.org (R.S.); nishikawa.yuma@molbiotech-nagoya.org (Y.N.); hnakano@agr.nagoya-u.ac.jp (H.N.)
* Correspondence: teruyo@agr.nagoya-u.ac.jp; Tel.: +81-52-789-4144

Abstract

Polyproline residues are well known to induce ribosomal stalling during translation. Our previous work demonstrated that inserting a short translation-enhancing peptide, Ser-Lys-Ile-Lys (SKIK), immediately upstream of such difficult-to-translate sequences can significantly alleviate ribosomal stalling in *Escherichia coli*. In this study, we provide a quantitative evaluation of its translational effect by kinetically analyzing the influence of the SKIK peptide on polyproline motifs using a reconstituted *E. coli* in vitro translation system. Translation rates estimated under reasonable assumptions fitted well to a Hill equation within a Michaelis–Menten-like kinetic framework. We further revealed that repetition of the SKIK tag did not provide any positive effect on translation. Moreover, introduction of the SKIK tag increased the production of polyproline-containing proteins, including human interleukin 11, human G protein signaling modulator 3, and DUF58 domain–containing protein from *Streptomyces* sp. in *E. coli* cell-free protein synthesis. These findings not only provide new insight into the fundamental regulation of translation by nascent peptides but also demonstrate the potential of the SKIK peptide as a practical tool for synthetic biology, offering a strategy to improve the production of difficult-to-express proteins.

Keywords: SKIK peptide; polyproline; translation; *Escherichia coli*; cell-free protein synthesis; difficult-to-express protein

check for updates

Academic Editor: Bernd Rehm

Received: 18 August 2025
Revised: 19 September 2025
Accepted: 28 September 2025
Published: 3 October 2025

Citation: Yoshino, A.; Shimoji, R.; Nishikawa, Y.; Nakano, H.; Ojima-Kato, T. Analysis and Application of Translation-Enhancing Peptides for Improved Production of Proteins Containing Polyproline. *SynBio* **2025**, *3*, 14. https://doi.org/10.3390/synbio3040014

Copyright: © 2025 by the authors. Licensee MDPI, Basel, Switzerland. This article is an open access article distributed under the terms and conditions of the Creative Commons Attribution (CC BY) license (https://creativecommons.org/licenses/by/4.0/).

1. Introduction

Protein synthesis, comprising the transcription of DNA into mRNA and the subsequent translation of mRNA into proteins by ribosomes, is fundamental to synthetic biology. Despite significant advances in the toolbox for recombinant protein production, many proteins remain difficult to express [1–3].

Ribosomal stalling during translation is a widespread phenomenon that can be triggered by specific nascent peptide sequences or amino acid motifs called arrest peptides (APs) [4,5]. Among these, consecutive proline residues—referred to as polyproline stretches—are well known to impede translation elongation by slowing peptide bond formation and perturbing ribosome dynamics in both eukaryotic and prokaryotic translation systems [6–9]. Such motifs are found across all domains of life, from bacterial envelope proteins to eukaryotic cytoskeletal regulators and signaling proteins, indicating their functional

importance. However, their presence can also present a major obstacle in heterologous protein expression systems.

Several strategies have been explored to alleviate ribosome stalling, including the use of elongation factor P (EF-P) and codon optimization [10–13]. Our previous work identified the SKIK peptide as a translation-enhancing tag that can reduce SecM- and polyproline-induced stalling in *E. coli*. This effect was observed in both in vivo and in vitro systems [14–16]. This tag has since been applied to improve recombinant protein yields in various contexts [17–21]. Although the precise mechanism remains unclear, our earlier findings suggest that its effect may involve nascent peptide–mediated modulation of ribosome dynamics rather than changes in mRNA structure alone [15].

In this study, we sought to gain quantitative insight into the influence of the SKIK tag on polyproline-induced ribosome stalling. Using a reconstituted *E. coli* cell-free translation system, we performed kinetic analyses of translation in the presence or absence of the SKIK tag. The resulting translation rate data were fitted to the Hill equation within a Michaelis–Menten–like kinetic framework to explore potential cooperative effects. We further examined the impact of SKIK repetition on translation efficiency and evaluated its utility for enhancing the production of polyproline-containing proteins, including human interleukin 11, human G protein signaling modulator 3, and DUF58 domain–containing protein from *Streptomyces* sp. These findings advance our understanding of short nascent peptide tags as tools to mitigate ribosome stalling and improve the productivity of difficult-to-express proteins.

2. Results

2.1. Effect of SKIK Peptide on Translation Kinetics

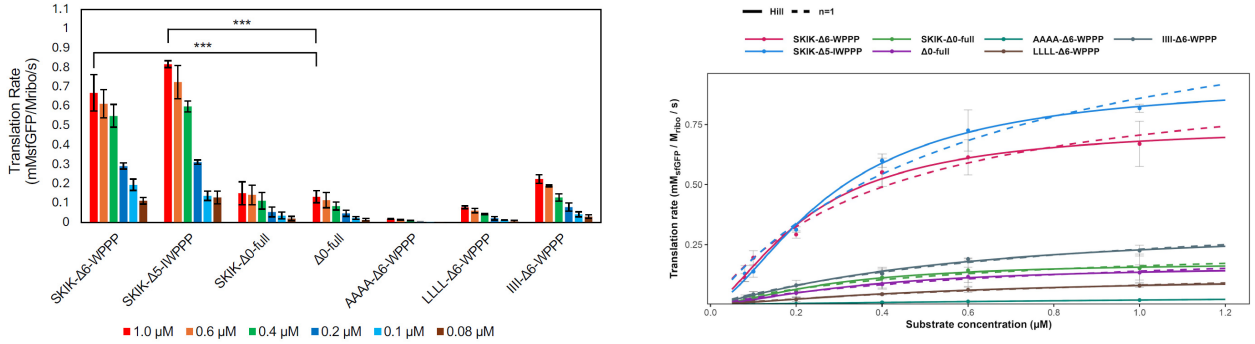
We performed a kinetic analysis to investigate how the SKIK tag influences translation of the WPPP AP (FQKYGIWPPP) and to elucidate its underlying mechanism of action. Seven constructs were designed and evaluated, comprising both SKIK-tagged and non-SKIK variants, as shown in Table 1. The SKIK-tagged constructs included SKIK-Δ6-WPPP, in which the SKIK tag was placed immediately upstream of the WPPP AP sequence with a six-residue N-terminal deletion, resulting in SKIK-WPPP-sfGFP-His; SKIK-Δ5-IWPPP, which contained a five-residue N-terminal deletion; and SKIK-Δ0-full, where the SKIK tag was fused to the intact full-length WPPP AP sequence. In our previous study [16], we systematically analyzed positional variants of the SKIK tag, including Δ1–Δ4. We found that placing the tag closer to the polyproline motif enhanced translation, with Δ5 showing the highest activity and Δ6 also retaining relatively high activity. Therefore, in the present work, we selected Δ5 and Δ6 as representative high-activity constructs for detailed kinetic comparison. The SKIK tag was encoded by TCTAAAATAAAA, because its codon usage does not affect SKIK-mediated translation enhancement, as shown in our previous study analyzing 36 synonymous variants in *E. coli* [15]. The non-SKIK constructs were Δ0-full, the full-length WPPP AP without the SKIK tag, and AAAA-Δ6-WPPP, LLLL-Δ6-WPPP, and IIII-Δ6-WPPP, in which the N-terminal four residues were replaced by AAAA, LLLL, and IIII, respectively. These peptides were chosen based on their codon families representing high- (AAAA encoded by GCA–GCT–GCC–GCG, = 83% GC), intermediate- (LLLL encoded by CTT–CTC–CTA–CTG, = 50% GC), and low- (IIII encoded by ATC–ATT–ATC–ATA, = 17% GC) GC usage. This design allowed us to investigate peptide-driven effects while minimizing potential bias from mRNA GC content or secondary structure. In all constructs, the "Δ" symbol denotes the number of amino acid residues removed from the N-terminus of the original WPPP AP (FQKYGIWPPP).

Table 1. Overview of sequences used in translational analysis.

Name	Tag	Polyproline-Containing Sequence
SKIK-Δ6-WPPP	SKIK	WPPP
SKIK-Δ5-IWPPP	SKIK	IWPPP
SKIK-Δ0-full	SKIK	FQKYGIWPPP
Δ0-full	-	FQKYGIWPPP
AAAA-Δ6-WPPP	AAAA	WPPP
LLLL-Δ6-WPPP	LLLL	WPPP
IIII-Δ6-WPPP	IIII	WPPP

All constructs contain sfGFP gene with His tag at the C-terminus in pET22b vector.

As shown in Figure 1a, constructs containing SKIK directly upstream of the polyproline motif—namely SKIK-Δ6-WPPP and SKIK-Δ5-IWPPP—exhibited significantly higher sfGFP fluorescence intensity than all other constructs over the full range of mRNA concentrations tested (0.08–1.0 μM). In contrast, SKIK-Δ0-full, in which the SKIK tag is positioned further from the polyproline motif, exhibited low-level fluorescence intensity that was comparable to that of Δ0-full (without SKIK). These results indicate that placing the SKIK tag immediately upstream of the proline-rich region tends to enhance translation efficiency, irrespective of mRNA concentration.



(**a**) (**b**)

Figure 1. Translation analysis: (**a**) translation rates of SKIK-tagged and non-tagged constructs were measured at different substrate (mRNA) concentrations (0.08–1 μM), with translation efficiency quantified by the fluorescence intensity of synthesized sfGFP. (**b**) shows measured translation rates (data points) along with fitted curves derived from the Hill equation, used for kinetic parameter estimation. For comparison, curves based on the Hill equation with a fixed coefficient (n = 1) are shown as dashed lines, whereas best-fit curves with variable Hill coefficients are shown as solid lines. Translation rates were calculated as the increase in sfGFP concentration (mM) normalized to ribosome concentration, per second, during the linear phase of the reaction. All data represent the mean ± SD from three independent experiments (n = 3). In panel (**a**), statistical significance was evaluated by one-way ANOVA followed by Dunnett's multiple comparison test, with SKIK-Δ6-WPPP and SKIK-Δ5-IWPPP compared to Δ0-full at 1.0 μM mRNA concentration. Significant differences are indicated as *** $p < 0.001$.

To quantify these effects, we modeled the translation kinetics using a Michaelis–Menten–like framework, treating mRNA as the substrate (S), sfGFP as the product (P), and the ribosome as the enzyme (E). For simplicity, the model was based on the following assumptions: (1) the sfGFP folding rate does not limit fluorescence signal output, (2) the cell-free translation system provides sufficient translational components without inhibitory factors, and (3) each ribosome remains bound to its mRNA until the full-length sfGFP is synthesized.

For convenience, the sfGFP production rate was taken as a proxy for the translation rate and modeled mathematically using the Hill equation—an extension of the Michaelis–Menten equation that incorporates cooperativity via the Hill coefficient (n). In this study, the Hill model was employed because it provided a better fit to the experimental data than the standard Michaelis–Menten model assuming $n = 1$, thereby allowing more accurate estimation of kinetic parameters including V_{max} (the maximum translation rate), K_d (the substrate concentration at half-maximal rate), and n (the Hill coefficient indicating the degree of cooperativity) [22,23].

As a simplified model, the translation process is represented by the following reaction model, where k_1 denotes the rate constant for formation of the ribosome–mRNA complex, and k_2 represents the rate of protein synthesis from this complex.

$$\mathrm{nS+E} \underset{k_2}{\overset{k_1}{\rightleftharpoons}} \mathrm{SnE} \xrightarrow{} \mathrm{P}$$

The translation rate v is expressed by the following equation (see Section 4.4 for detailed derivation).

$$v = \frac{V_{max}\ [S]^n}{{K_d}^n + [S]^n}\ (K_d = \frac{k_2}{k_1})$$

This model yields a Hill-type equation, which describes the relationship between mRNA concentration and the rate of translation.

Based on the Hill equation described above, the measured translation rates of SKIK-Δ6-WPPP and SKIK-Δ5-IWPPP were fitted to the model. In this analysis, nonlinear least-squares regression was performed in R using mRNA as the substrate, and this fitting approach was applied to all constructs to evaluate their translation kinetics (Figure 1b). The protocol for the fitting procedure is described in Section 4.

As the concentration of mRNA increased, the translation rate exhibited a corresponding increase for all constructs. However, the rate of increase gradually diminished at higher concentrations, resulting in typical saturation curves. When the data were fitted to these kinetic profiles, the Hill model—which allows the Hill coefficient (n) to vary—provided a superior fit in comparison to the conventional Michaelis–Menten model, which assumes $n = 1$.

Table 2 summarizes the kinetic parameters for translational efficiency derived using the Hill equation analysis and provides the absolute values of each kinetic parameter (V_{max}, K_d, k_1, k_2, and n) for all constructs. The SKIK-tagged constructs, SKIK-Δ6-WPPP and SKIK-Δ5-IWPPP, exhibited significantly higher V_{max} values of (0.752 and 0.936, respectively) compared with Δ0-full control (0.165), corresponding to 4.56- and 5.67-fold increases. Both k_1 and k_2 values increased to 1.614 and 0.376 for SKIK-Δ6-WPPP and to 1.624 and 0.468 for SKIK-Δ5-IWPPP, whereas the Δ0-full without SKIK tag showed only 0.227 and 0.082, respectively. To summarize these, k_1 and k_2 increased ~7-fold and ~4–5-fold by SKIK tag, respectively, indicating that the presence of the SKIK tag substantially accelerates both the initiation- and elongation-related kinetic rate constants.

Although the primary focus of this study was on the WPPP AP, we also reanalyzed the kinetic parameters for constructs containing another AP, SecM AP (FSTPVWISQAQGIRAGP), using data from our previous work [16]. Applying the same Hill fitting approach used for the WPPP variants yielded V_{max} values of 0.213 (non-tagged SecM AP) and 3.01 (SKIK-tagged SecM AP), with Hill coefficients (n) of 0.978 and 1.42, respectively. Direct comparison under identical analytical conditions revealed that polyproline-containing constructs in this study exhibited lower V_{max} values (e.g., 0.936 for SKIK-Δ5-IWPPP and 0.165 for Δ0-full; Table 2).

Table 2. Kinetic parameters calculated from nonlinear regression based on Hill equation.

	V_{max}	K_d	k_1	k_2	n
SKIK-Δ6-WPPP	0.752	0.233	1.614	0.376	1.546
SKIK-Δ5-IWPPP	0.936	0.288	1.624	0.468	1.621
SKIK-Δ0-full	0.176	0.286	0.309	0.088	1.601
Δ0-full	0.165	0.364	0.227	0.082	1.489
AAAA-Δ6-WPPP	0.096	4.170	0.011	0.048	0.969
LLLL-Δ6-WPPP	0.122	0.613	0.099	0.061	1.308
IIII-Δ6-WPPP	0.334	0.531	0.315	0.167	1.201

Values were derived from nonlinear regression of translation kinetics.

2.2. Effect of Repetitive SKIK on Translation

To investigate the effect of repetitive SKIK sequences on translation, plasmids pET22b-SKIK-IWPPP-sfGFP-6×His containing a single SKIK tag and pET22b-$(SKIK)_x$-IWPPP-sfGFP-6×His containing two or three repetitive SKIK tags (x = 2, 3) were constructed. The translation-enhancing effects were evaluated in both in vitro and in vivo expression systems, based on the amount of sfGFP synthesized.

The sfGFP fluorescence intensity obtained from in vitro translation using a cell-free protein synthesis (CFPS) system and mRNA as the template was normalized by setting the positive control to 1. The average values of relative intensities are shown in Figure 2a. For in vivo expression in *E. coli* BL21(DE3) cells, the sfGFP fluorescence intensity was normalized to the total protein concentration and then to the sfGFP positive control, as shown in Figure 2b.

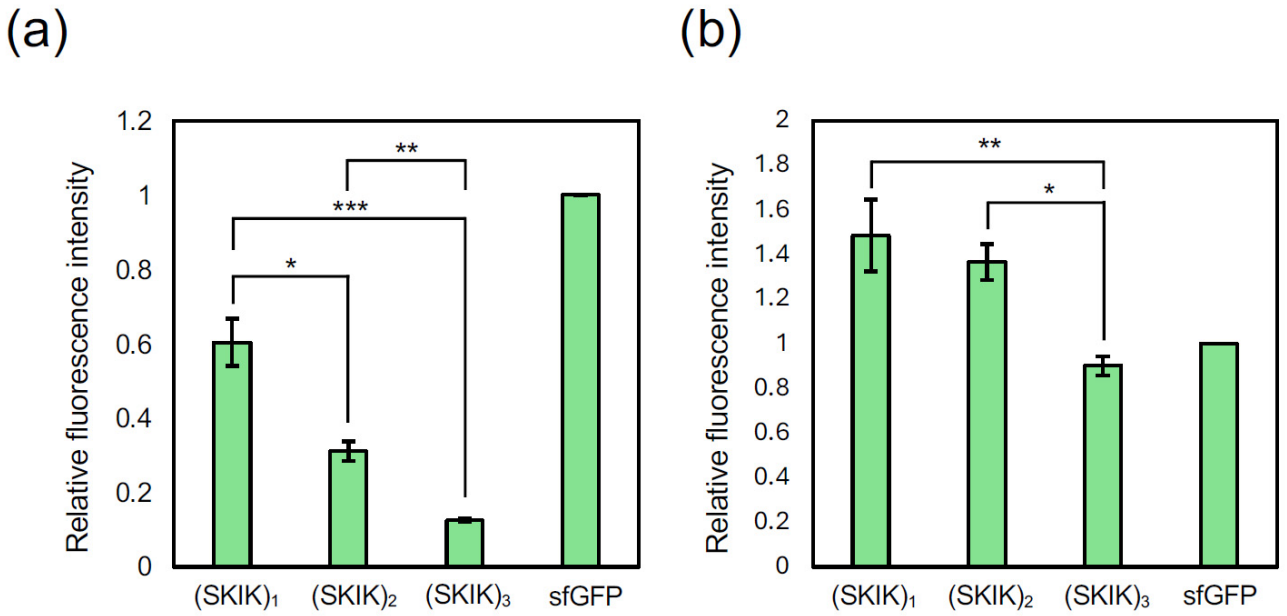
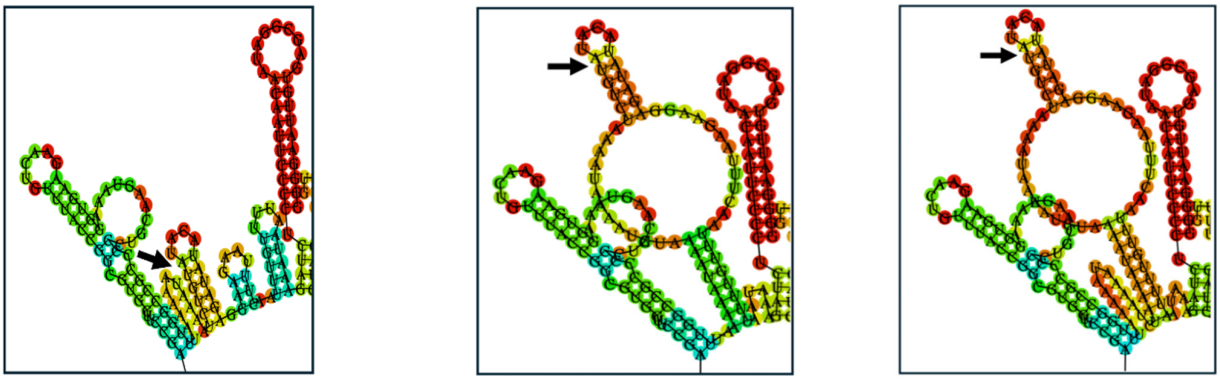


Figure 2. Effect of N-terminal SKIK repeats on sfGFP expression in vitro and in vivo. (**a**) In vitro translation using a CFPS system. Fluorescence intensity of sfGFP was measured for each construct with different N-terminal sequences: single, double, and triple SKIK repeats ($(SKIK)_1$, $(SKIK)_2$, $(SKIK)_3$) attached to IWPPP-sfGFP. The sfGFP construct without any additional tags was utilized as a reference, and all fluorescence values are normalized to that of untagged sfGFP. (**b**) In vivo expression in *E. coli* BL21(DE3) cells. Fluorescence intensity of sfGFP for each construct is presented as relative fluorescence intensity normalized to untagged sfGFP. Each bar represents the mean ± SD from three independent replicates (n = 3). Statistical significance was evaluated by one-way ANOVA followed by Tukey's multiple comparison test. Significant differences are indicated as * $p < 0.05$, ** $p < 0.01$, and *** $p < 0.001$.

In both cell-free and cellular systems, the construct with a single SKIK tag exhibited the highest expression level, while the expression decreased as the number of SKIK repeats increased. These results indicate that repeating the SKIK sequence does not show any positive effect on the translation-enhancing strength.

To investigate the cause of the reduced translation efficiency observed with increasing SKIK repeats, we examined the predicted mRNA secondary structures around the translation initiation region (Figure 3). The minimum free energy (ΔG) values for the −30 to +50 nucleotide region relative to the AUG start codon were −11.2 kcal/mol for IWPPP-sfGFP without SKIK and −8.80 kcal/mol, −6.00 kcal/mol, and −4.90 kcal/mol for constructs containing $(SKIK)_1$, $(SKIK)_2$, and $(SKIK)_3$, respectively.



(**a**) (**b**) (**c**)

Figure 3. RNA secondary structures near the start codon and local folding energies for constructs with different numbers of SKIK tags. (**a**–**c**) Predicted minimum free energy (MFE) RNA secondary structures of mRNAs containing (**a**) one, (**b**) two, or (**c**) three repeated SKIK tags. Structures were predicted using the full-length mRNA sequences, but only the region near the start codon (AUG) is shown. The black arrows indicate the position of the AUG codon. Each circle represents a nucleotide, and base pairs are indicated by connecting lines. The color gradient (from red to blue) reflects the confidence of base-pair formation, with red indicating high probability. Both the secondary structures and the ΔG values were calculated using the RNAfold web server (http://rna.tbi.univie.ac.at/cgi-bin/RNAWebSuite/RNAfold.cgi (accessed on 26 July 2025)).

2.3. Application of SKIK on Improved Production of Proteins Containing Polyproline

Finally, to examine the effect of SKIK on the expression of natural proteins containing polyproline sequences near the N-terminus, we selected three model proteins (see Section 4 for details). SKIK was introduced under two conditions: (I) immediately upstream of the polyproline stretch (Direct) and (II) immediately after the initiation methionine (N-terminus). Protein synthesis was carried out using a CFPS system, and expression levels were analyzed by Western blotting (Figure 4).

For IL-11, the SKIK-tagged construct exhibited a higher protein production compared to the construct without SKIK. In the case of GPSM3, the Direct SKIK construct showed little to no difference in protein production compared to the untagged version, whereas the N-terminus SKIK construct resulted in higher production levels than both constructs. Notably, the N-terminal SKIK tagged GPSM3 showed two additional lower-molecular-weight bands at 17.2 kDa and 14.4 kDa in addition to the main band (19.1 kDa) corresponding to the correct size. For DUF58, the construct lacking SKIK only yielded a band at the unexpected molecular weight of 33.6 kDa, whereas the SKIK-tagged construct produced a band corresponding to the anticipated molecular weight of DUF58 (48.9 kDa).

These results suggest that the introduction of the SKIK tag can improve both the expression level and translational accuracy of difficult-to-express proteins. The effect

of the SKIK tag appears to depend on the type of protein and the position at which it is introduced.

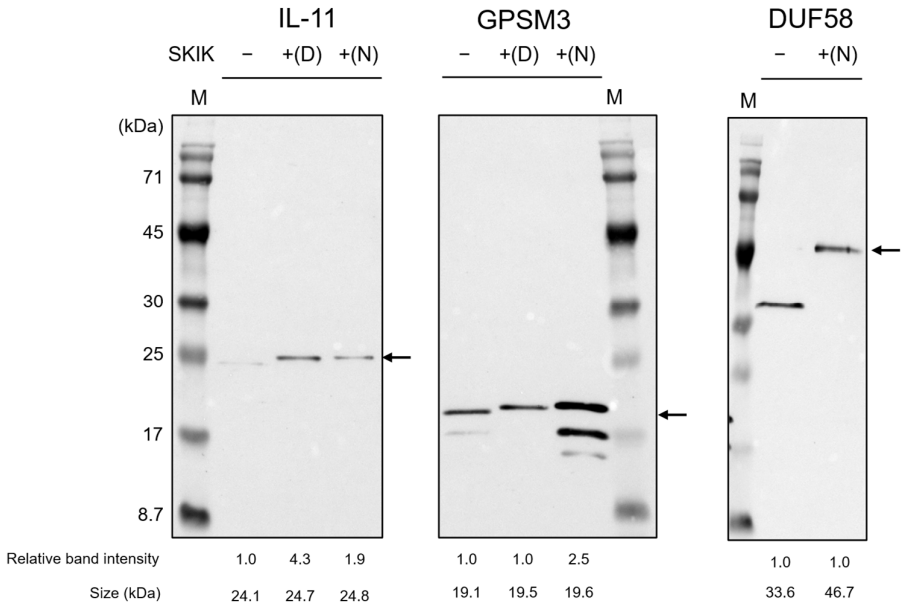


Figure 4. Effect of SKIK tagging on the expression of polyproline-containing proteins: Western blot analysis of IL-11, GPSM3, and DUF58 constructs expressed in a CFPS system. Constructs contain either no tag, Direct SKIK (+(D)), or N-terminal SKIK (+(N)). Band intensities relative to untagged constructs and their molecular weights calculated using Image Lab software are shown under the gel image. Arrows indicate theoretical molecular weights based on the sequence information.

3. Discussion

3.1. Effect of SKIK Peptide on Translation Kinetics of Polyproline Containing AP

Attachment of the SKIK tag to the full-length WPPP AP sequence, FQKYGIWPPP, did not significantly alter the translation rates compared with the SKIK-free construct (SKIK-Δ0-full vs. Δ0-full; Figure 1). In contrast, placing SKIK in closer proximity to the polyproline motif, as in SKIK-Δ6-WPPP and SKIK-Δ5-IWPPP, resulted in higher V_{max} values—4.56- and 5.67-fold greater, respectively, and raised both translation rate constants k_1 and k_2 by approximately sevenfold and fivefold relative to Δ0-full (Figure 1 and Table 2). These results indicate that SKIK positioned close to the WPPP motif effectively alleviates polyproline-induced ribosomal stalling [16].

The observed increases in the translation rate constants suggest two possible mechanisms: (1) an increase in k_1, representing enhanced formation of ribosome–mRNA complexes ready to start translation, which may indicate that ribosomes bind more readily to the mRNA, and (2) an increase in k_2, indicating a higher rate of productive translation, likely due to the reduced time from initiation to termination. Together, these results suggest that SKIK attachment can enhance overall translational efficiency, potentially by accelerating ribosome recycling, consistent with our previous findings [16].

The Hill coefficient (n) obtained from curve fitting offers insight into ribosome behavior by reflecting the degree of cooperativity—how the binding of one ribosome might influence the recruitment or activity of others. While $n > 1$ suggests positive cooperativity and provides a lower bound for the number of interacting sites, and $n < 1$ may indicate negative cooperativity, the coefficient itself does not directly indicate the actual number of ribosome-binding sites [24–26]. For example, hemoglobin has four oxygen-binding sites but shows reported Hill coefficients between 1.7 and 3.2. In this study, elevated n values in SKIK-tagged constructs could imply cooperative ribosome binding to mRNA; however, this

interpretation remains hypothetical and requires further validation through direct assays such as ribosome profiling. Here, n is primarily used as an empirical fitting parameter to capture the sigmoidal shape of the translation response curves rather than as definitive proof of cooperativity. Although not in the context of ribosome–mRNA interactions, this empirical use of the Hill coefficient is consistent with previous studies, where the Hill model was applied primarily as a better fitting approach when Michaelis–Menten kinetics did not adequately describe the experimental data [27].

While polyproline and SecM APs are both well-studied stalling elements, their relative stalling strength has rarely been quantified directly. Existing approaches—such as reporter assays, ribosome profiling, or structural studies—typically provide qualitative rather than numerical comparisons [12,28,29]. By applying Hill equation–based kinetic modeling, we obtained absolute parameters (V_{max}, k_1, k_2) under identical conditions, enabling a side-by-side comparison of WPPP polyproline and SecM APs. This approach will offer a general framework for quantitatively comparing the stalling strength across sequences, addressing a current methodological gap in the field.

3.2. Effect of Repetitive SKIK on Translation

We investigated the effect of SKIK repeats on translation for the first time and unexpectedly found that apparent translation efficiency decreased as the number of repeats increased in both in vitro and in vivo systems (Figure 2). RNAfold predictions for the region surrounding the start codon (−30 to +50 nt) indicated that a single SKIK tag $(SKIK)_1$ forms relatively simple, open structures, whereas $(SKIK)_2$ and $(SKIK)_3$ generate more complex and stable local structures that may hinder ribosome access (Figure 3). We also carried out predictions using CentroidFold [30] (see Supplementary Figure S1). Although the calculated ΔG values became higher with increasing SKIK repeats, this trend was inversely correlated with protein expression levels, suggesting that specific local structures near the start codon may be more influential than the overall ΔG.

Generally, mRNAs with higher ΔG values (weaker secondary structures) are considered less likely to obstruct ribosomal translation initiation. However, paradoxical findings from yeast in vitro studies have shown increased protein yields from mRNAs with lower ΔG values [31]. In addition, Bao et al. reported that discrete structural motifs, rather than bulk stability, can influence the translation elongation efficiency [32]. Our previous work also demonstrated that the translation-enhancing effect of a single SKIK tag is driven by the nascent peptide rather than changes in mRNA secondary structure [15]. Taken together, these results suggest that while a single SKIK tag can promote translation via a nascent-peptide–mediated mechanism, multiple SKIK repeats may override this benefit by introducing inhibitory RNA structures in the vicinity of the start codon.

3.3. Application of SKIK on Improved Production of Proteins Containing Polyproline

To assess the applicability of the SKIK translation-enhancing peptide to proteins containing polyproline motifs, we compared two tag positions: directly upstream of the polyproline sequence (“Direct”) and immediately after the initiation codon (“N-terminus”). In IL-11, the Direct construct yielded elevated expression while N-terminus in GPSM3 demonstrated most enhanced efficacy (Figure 4). This suggests that the optimal position for SKIK tagging may differ depending on the target protein. An unexpected feature was observed for the N-terminal SKIK–GPSM3 construct, which produced additional lower-molecular-weight bands besides the correct main product. As this Western blotting analysis detected the C-terminal His tag, these smaller bands are likely byproducts starting from unexpected internal codons or truncated products after translation. This aligns with

previous reports showing that N-terminal amino acid changes can strongly influence the translation efficiency [33,34].

For DUF58, the full-length product was detected only when SKIK was added at the N-terminus, while the untagged construct yielded a smaller byproduct. The DUF58 gene contains a non-canonical start codon (UUG) near a potential internal initiation region, yet RNAfold predictions revealed no significant hairpin structures occluding the canonical start codon. The origin of the aberrant band in the untagged construct remains unclear, but clarifying the translation initiation site will require N-terminal sequencing or mass spectrometry analysis [35,36]. In any case, SKIK tagging clearly increased production of the correctly translated DUF58 protein.

These results demonstrate that SKIK can substantially improve protein yields in *E. coli* CFPS systems for challenging targets, including human and actinobacterial genes with polyproline sequences. Importantly, they highlight that the optimal tag position is not universal and must be empirically determined for each target. This positional dependency is consistent with prior studies showing that even subtle changes in N-terminal sequence context can have profound effects on translation initiation and elongation efficiency [34,35]. The present findings thus expand the utility of SKIK tagging from in vitro model systems to more complex, translationally challenging proteins, providing a practical strategy for boosting expression of difficult targets in synthetic biology and protein engineering.

4. Materials and Methods

4.1. Construction of Plasmid DNA for Kinetic Analysis

The plasmid pET22b-SKIK-WPPP-sfGFP-His and its derivatives shown in Table 1 were originally constructed in a previous study by Nishikawa et al. [16]. They were used in kinetic analyses and experiments investigating the effects of consecutive proline sequences. To investigate the effect of repeated SKIK sequences on ribosomal stalling caused by the peptide sequence IWPPP, single-stranded DNA oligonucleotides encoding one, two, or three tandem SKIK repeats were assembled with double-stranded DNA fragments immediately upstream of the IWPPP coding region using the HiFi DNA assembly technique. The assembled plasmids were transformed into *E. coli* XL10-Gold competent cells. Plasmid DNA with the correct sequence was extracted from overnight LB cultures using the FastGene Plasmid Mini Kit (Nippon Genetics Co., Ltd., Bunkyo-ku, Tokyo). Unless otherwise noted, all media were supplemented with 100 μg/mL ampicillin.

4.2. Construction of Plasmid DNA for Expressing Polyproline Containing Genes

To assess the effect of SKIK insertions on protein production, three genes encoding polyproline motifs or proline-rich sequences near the N-terminus were arbitrarily selected from GenBank. Codon-optimized synthetic genes were ordered as gBlocks from Integrated DNA Technologies (Coralville, IA, USA). The first gene encodes human interleukin-11 (IL-11, Gene ID: 3589), a 121-amino acid cytokine belonging to the gp130 family. It contains a polyproline-rich motif (“PGP-PPG-PPP”) near its N-terminus and is involved in B cell maturation and the proliferation of hematopoietic cells [37]. The second gene encodes human G protein signaling modulator 3 (GPSM3, Gene ID: 63940), which is 125 amino acids in length and includes polyproline motifs “WPPP” and “PPPP” at residues 20 and 37, respectively. GPSM3 is predicted to act as a GTPase regulator and may participate in inflammation-related signaling pathways [38]. The third gene encodes a DUF58 domain-containing protein from *Streptomyces* sp. (GenBank ID: WP_129839319.1), consisting of 459 amino acids. This protein contains a “WPPPP” motif at position 3 and a “PPP” motif at position 14. While the DUF58 protein family remains uncharacterized, homologs have been identified in various bacterial and archaeal genomes, suggesting a conserved but yet

undefined function [39]. These genes and their corresponding amino acid residues are shown in Table S1.

Each gene with His tag at the C-terminus was individually cloned into a pET22b vector; then, insertion of the SKIK tag at upstream of specific polyproline sites was carried out by using whole-plasmid PCR using site-specific primers (Table S2) and KOD One (Toyobo, Osaka, Japan), a high-fidelity DNA polymerase, under the following conditions: initial denaturation at 94 °C for 1 min; 35 cycles of 98 °C for 10 s, 55 °C for 5 s, and 68 °C for 1 min; then held at 12 °C. *Dpn*I-treated PCR products were introduced to XL10-gold strains, and plasmids were extracted as described above. A total of eight variants were constructed and are summarized in Supplementary Table S1.

The DNA fragments containing the T7 promoter and terminator sequences for CFPS were amplified by PCR using the primer pair F1 and R1 (Table S2), with the constructed plasmids serving as templates. The PCR was performed with KOD One DNA polymerase under the following thermal cycling conditions: initial denaturation at 98 °C for 1 min; 30 cycles of denaturation at 98 °C for 10 s, annealing at 50 °C for 5 s, and extension at 68 °C for 30 s; followed by a final extension at 68 °C for 1 min, and a hold at 12 °C. The resulting PCR products were purified using a silica column-based DNA purification kit and subsequently utilized as templates for in vitro transcription.

4.3. Cell-Free Translation

In vitro transcription was conducted using the T7 RiboMAX™ Large Scale RNA Production System (Promega, Madison, WI, USA), according to the manufacturer's instructions. The transcribed mRNAs were purified using the NucleoSpin RNA Plus kit (Takara Bio, Kusatsu, Japan). The concentration of each mRNA sample was subsequently measured with a NanoDrop One spectrophotometer (Thermo Fisher Scientific, Waltham, MA, USA). To calculate the molecular weight of each sample, we used the RNA Molecular Weight Calculator provided by AAT Bioquest (https://www.aatbio.com (accessed on 27 March 2025)). For translational kinetic analysis, CFPS reactions were carried out using PUREfrex® 2.1 (GeneFrontier Corporation, Kashiwa, Japan) in a total volume of 10 µL. Each reaction contained 4.0 µL of Solution I, 0.5 µL of Solution II, 1.0 µL of Solution III (20 µM ribosomes), 0.8 µL of 10 mM cysteine, and 0.7 µL of RNase inhibitor (Toyobo, Osaka, Japan). Template mRNA was added at appropriate concentrations according to the experimental design. The reactions were monitored in real time using a CFX Opus 96 Real-Time PCR System (Bio-Rad, Hercules, CA, USA) at 37 °C for 90 min. The fluorescence intensity of synthesized sfGFP was measured at one-minute intervals after an initial 30 s incubation. To convert fluorescence signals into sfGFP concentrations, a standard curve was prepared using purified sfGFP at concentrations of 10, 1, 0.1, 0.01, and 0.001 µM. The translation rate—defined as the amount of sfGFP produced normalized by ribosome concentration (M), per unit time—was determined from the slope of the fluorescence increase during the linear phase of the reaction, where the rate was at its maximum and remained consistent across all samples.

4.4. Derivation of the Hill Equation and Kinetic Analysis

According to the principles of mass-action kinetics, the rate of formation and dissociation of the $[SnE]$ complex is described by the following equation:

$$\frac{d[SnE]}{dt} = k_1[S]^n[E] - k_2[SnE].$$

Assuming the steady-state approximation, under which the concentration of the intermediate complex [SnE] remains constant over time, the following equation is derived:

$$\frac{d[SnE]}{dt} = 0 \implies [SnE] = \frac{k_1}{k_2}[S]^n[E].$$

The total concentration of ribosomes (E) is expressed as follows:

$$[E_{total}] = [E] + [SnE].$$

Solving for [E] and substituting into the aforementioned expression yields

$$[SnE] = \frac{k_1}{k_2}[S]^n([E_{total}] - [SnE]).$$

In this case, the apparent dissociation constant is expressed as

$${K_d}^n = \frac{k_2}{k_1}.$$

By substituting this definition into the previous equation, we obtain

$$[SnE] = \frac{[S]^n([E_{total}] - [SnE])}{{K_d}^n}.$$

Rearranging terms to isolate [SnE] leads to

$$[SnE](\frac{{K_d}^n + [S]^n}{{K_d}^n}) = \frac{[S]^n[E_{total}]}{{K_d}^n}.$$

Dividing both sides by $1 + \frac{[S]^n}{{K_d}^n}$ yields

$$[SnE] = \frac{\frac{[S]^n[E_{total}]}{{K_d}^n}}{\frac{{K_d}^n + [S]^n}{{K_d}^n}},$$

which simplifies to

$$[SnE] = \frac{[E_{total}][S]^n}{{K_d}^n + [S]^n}.$$

Given the definition of $V_{max} = k_{cat}$ [E_{total}] and assuming that the translation rate v is proportional to the concentration of the active complex [SnE], the following equation is obtained:

$$v = k_{cat}[SnE] = \frac{V_{max}[S]^n}{{K_d}^n + [S]^n}$$

These derivations follow the classical Michaelis–Menten and Hill formulations [16,23,25].

The translation rate data were analyzed using nonlinear least-squares regression with the nlsLM function from the minpack.lm package in R (version 4.4.3), as part of a multifaceted quantitative approach. This analysis enabled curve fitting to the Hill equation (y = $V_{max} \times S^n/({K_d}^n + S^n)$), yielding key parameters: the maximum translation rate (V_{max}), the half-maximal concentration (K_d), and the Hill coefficient (n). The generation of graphs was accomplished through the utilization of the ggplot2 package (version 3.5.2), with error bars denoting standard deviations (n = 3).

To evaluate the effect of the SKIK peptide on the synthesis of proteins containing polyproline motifs, reactions were performed under the same conditions as described above, except that DNA fragments were used as templates instead of mRNA.

4.5. Expression in E. coli BL21(DE3)

To assess the SKIK repeat, expression in *E. coli* BL21(DE3) was carried out using autoinduction. Terrific broth (Bacto tryptone, 12 g; yeast extract, 24 g; KH_2PO_4, 6.8 g; $Na_2PO_4 \cdot 12H_2O$, 7.1 g; $MgSO_4$, 0.15 g; $(NH_4)_2SO_4$, 2.58 g; 1% (*w*/*v*) glucose, 5 mL; and 8% (*w*/*v*) lactose; 25 mL, per 1 L, adjusted pH 7.4) was used as the autoinduction medium. Single colonies were inoculated into 4 mL of LB medium and grown overnight at 37 °C with shaking. Then, aliquots (50 μL) were transferred into 3 mL of Terrific broth and cultured at 30 °C until the OD600 reached 0.4 to 0.6. The cells were harvested by centrifugation and washed with PBS, and the OD600 of each sample was adjusted to the same level by diluting with PBS. The same number of cells from each sample were lysed using *E. coli*/Yeast Protein Extraction Buffer (Tokyo Chemical Industry, Tokyo, Japan) according to the manufacturer's instructions. The extracted soluble fraction containing the produced sfGFP was analyzed by SDS-PAGE and micro plate reader (Tecan Infinite 200 pro (Tecan, Maennedorf, Switzerland), excitation 485 nm (band width 9 nm)/emission 535 nm (band width 20 nm)).

4.6. SDS-PAGE and Quantification of the Proteins by Western Blotting

For each sample, 3 μL (IL-11 and GPSM3) or 5 μL (DUF58) of CFPS product was mixed with DTT (10 mM final concentration), sample loading buffer, and water, then heated at 98 °C for 3 min using a heat block, and subjected to SDS-PAGE (12.5% polyacrylamide). The gel and nitrocellulose membrane were soaked in blotting buffer (25 mM Tris, 192 mM Glycine, 20% MeOH) and then transferred using a Trans-Blot SD cell (Bio rad, Hercules, CA, USA) at 10 V for 30 min. After transfer, the membrane was washed with PBST and blocked using 1% skim milk (Nacalai Tesque, Kyoto, Japan) dissolved in PBST, for 60 min. The membrane was incubated with a 1:2500 diluted Anti-His tag monoclonal antibody-HRP conjugation (MBL, Nagoya, Japan) for 60 min at room temperature, followed by washes with PBST three times. The substrate, 1-Step™ Ultra TMB-Blotting Solution (Thermo, Waltham, WA, USA), was added until color development was observed, and the membrane was then washed with deionized water. After color development, the membrane image was captured using the ChemiDoc™ MP Imaging System (Bio-Rad, Hercules, CA, USA). Both band intensities and molecular weights were analyzed using Image Lab software (Bio-Rad), based on the migration distance of marker proteins (Protein MultiColor Stable II, Large; Funakoshi, Tokyo, Japan).

5. Conclusions

In this study, we examined how the SKIK translation-enhancing peptide influences the translation of proteins containing polyproline sequences, a known cause of ribosomal stalling. Kinetic analyses in an *E. coli* cell-free system revealed that SKIK tagging increases both the rate of ribosome–mRNA complex formation and the rate of productive translation, effectively alleviating polyproline-induced stalling. We also found that repeating the SKIK motif did not further enhance translation. Applying SKIK tagging to natural proteins with polyproline sequences significantly improved their production, although the optimal tag position was protein-dependent. Importantly, our kinetic framework also enabled a numerical comparison of the stalling strength between different APs, suggesting a potential approach for quantitatively evaluating ribosomal stalling in future studies. These findings highlight SKIK tagging as a practical and versatile strategy for improving the production of difficult-to-express proteins, with potential applications in synthetic biology and protein engineering.

Supplementary Materials: The following supporting information can be downloaded at: https://doi.org/10.5281/zenodo.16892395, Table S1: Synthetic genes used in this study; Table S2: Primers used in this study. Sequence information of plasmids constructed in this study are provided as GenBank format; Figure S1: mRNA secondary structure predictions using CentroidFold.

Author Contributions: Conceptualization, T.O.-K.; methodology, T.O.-K., A.Y. and H.N.; investigation, A.Y., R.S. and Y.N.; writing—original draft preparation, A.Y.; writing—review and editing, T.O.-K. and H.N.; visualization, A.Y. and T.O.-K.; supervision, T.O.-K.; project administration, T.O.-K.; funding acquisition, T.O.-K. All authors have read and agreed to the published version of the manuscript.

Funding: This research was funded by the Japan Science and Technology agency FOREST Program (grant No. JPMJFR2204), GteXProgram Japan (grant numbers JPMJGX23B6 and JPMJGX23B4), and Japan Society for the Promotion for Science (grant number KAKENHI 23K04989).

Institutional Review Board Statement: Not applicable.

Informed Consent Statement: Not applicable.

Data Availability Statement: The original contributions presented in this study are included in the article and Supplementary Material. Further inquiries can be directed to the corresponding author.

Acknowledgments: The PUREfrex 2.1 used in this study was kindly provided by GeneFrontier Corporation. We would like to thank Takashi Kanamori. During the preparation of manuscript, the authors used ChatGPT-5 and DeepL Write (https://www.deepl.com/ja/write (accessed on 18 September 2025)) for language editing. ChatGPT-5 was also used to help draft the R code for Figure 1b. The authors have reviewed and edited the output and take full responsibility for the content of this publication.

Conflicts of Interest: The authors declare no conflicts of interest.

Abbreviations

The following abbreviations are used in this manuscript:

AP	Arrest peptide
CFPS	Cell-free protein synthesis

References

1. Li, Z.M.; Fan, Z.L.; Wang, X.Y.; Wang, T.Y. Factors Affecting the Expression of Recombinant Protein and Improvement Strategies in Chinese Hamster Ovary Cells. *Front. Bioeng. Biotechnol.* **2022**, *10*, 880155. [CrossRef] [PubMed]
2. Kim, K.; Choe, D.; Lee, D.H.; Cho, B.K. Engineering Biology to Construct Microbial Chassis for the Production of Difficult-to-Express Proteins. *Int. J. Mol. Sci.* **2020**, *21*, 990. [CrossRef] [PubMed]
3. Maltais, J.S.; Lord-Dufour, S.; Morasse, A.; Stuible, M.; Loignon, M.; Durocher, Y. Repressing Expression of Difficult-to-Express Recombinant Proteins during the Selection Process Increases Productivity of CHO Stable Pools. *Biotechnol. Bioeng.* **2023**, *120*, 2840–2852. [CrossRef] [PubMed]
4. Nakatogawa, H.; Ito, K. The Ribosomal Exit Tunnel Functions as a Discriminating Gate. *Cell* **2002**, *108*, 629–636. [CrossRef]
5. Ito, K.; Chiba, S. Arrest Peptides: Cis-Acting Modulators of Translation. *Annu. Rev. Biochem.* **2013**, *82*, 171–202. [CrossRef]
6. Pavlov, M.Y.; Watts, R.E.; Tan, Z.; Cornish, V.W.; Ehrenberg, M.; Forster, A.C. Slow Peptide Bond Formation by Proline and Other N-Alkylamino Acids in Translation. *Proc. Natl. Acad. Sci. USA* **2009**, *106*, 50–54. [CrossRef]
7. Peil, L.; Starosta, A.L.; Lassak, J.; Atkinson, G.C.; Virumäe, K.; Spitzer, M.; Tenson, T.; Jung, K.; Remme, J.; Wilson, D.N. Distinct XPPX Sequence Motifs Induce Ribosome Stalling, Which Is Rescued by the Translation Elongation Factor EF-P. *Proc. Natl. Acad. Sci. USA* **2013**, *110*, 15265–15270. [CrossRef]
8. Woolstenhulme, C.J.; Parajuli, S.; Healey, D.W.; Valverde, D.P.; Petersen, E.N.; Starosta, A.L.; Guydosh, N.R.; Johnson, W.E.; Wilson, D.N.; Buskirk, A.R. Nascent Peptides That Block Protein Synthesis in Bacteria. *Proc. Natl. Acad. Sci. USA* **2013**, *110*, E878–E887. [CrossRef]
9. Nagai, R.; Xu, Y.; Liu, C.; Shimabukuro, A.; Takeuchi-Tomita, N. In Vitro Reconstitution of Yeast Translation System Capable of Synthesizing Long Polypeptide and Recapitulating Programmed Ribosome Stalling. *Methods Protoc.* **2021**, *4*, 45. [CrossRef]

10. Krafczyk, R.; Qi, F.; Sieber, A.; Mehler, J.; Jung, K.; Frishman, D.; Lassak, J. Proline Codon Pair Selection Determines Ribosome Pausing Strength and Translation Efficiency in Bacteria. *Commun. Biol.* **2021**, *4*, 589. [CrossRef]
11. Doerfel, L.K.; Wohlgemuth, I.; Kothe, C.; Peske, F.; Urlaub, H.; Rodnina, M.V. EF-P Is Essential for Rapid Synthesis of Proteins Containing Consecutive Proline Residues. *Science* **2013**, *339*, 85–88. [CrossRef]
12. Huter, P.; Arenz, S.; Bock, L.V.; Graf, M.; Frister, J.O.; Heuer, A.; Peil, L.; Starosta, A.L.; Wohlgemuth, I.; Peske, F.; et al. Structural Basis for Polyproline-Mediated Ribosome Stalling and Rescue by the Translation Elongation Factor EF-P. *Mol. Cell* **2017**, *68*, 515–527.e6. [CrossRef] [PubMed]
13. Katoh, T.; Wohlgemuth, I.; Nagano, M.; Rodnina, M.V.; Suga, H. Essential Structural Elements in TRNAPro for EF-P-Mediated Alleviation of Translation Stalling. *Nat. Commun.* **2016**, *7*, 11657. [CrossRef] [PubMed]
14. Ojima-Kato, T.; Nagai, S.; Nakano, H. N-Terminal SKIK Peptide Tag Markedly Improves Expression of Difficult-to-Express Proteins in Escherichia Coli and Saccharomyces Cerevisiae. *J. Biosci. Bioeng.* **2017**, *123*, 540–546. [CrossRef] [PubMed]
15. Ojima-Kato, T.; Nishikawa, Y.; Furukawa, Y.; Kojima, T.; Nakano, H. Nascent MSKIK Peptide Cancels Ribosomal Stalling by Arrest Peptides in Escherichia Coli. *J. Biol. Chem.* **2023**, *299*, 104676. [CrossRef]
16. Nishikawa, Y.; Fujikawa, R.; Nakano, H.; Kanamori, T.; Ojima-Kato, T. Effect of Translation-Enhancing Nascent SKIK Peptide on the Arrest Peptides Containing Consecutive Proline. *ACS Synth. Biol.* **2024**, *13*, 3908–3916. [CrossRef]
17. Ojima-Kato, T.; Nagai, S.; Nakano, H. Ecobody Technology: Rapid Monoclonal Antibody Screening Method from Single B Cells Using Cell-Free Protein Synthesis for Antigen-Binding Fragment Formation. *Sci. Rep.* **2017**, *7*, 13979. [CrossRef]
18. Ojima-Kato, T. Advances in Recombinant Protein Production in Microorganisms and Functional Peptide Tags. *Biosci. Biotechnol. Biochem.* **2024**, *89*, 1–10. [CrossRef]
19. Wang, S.; Zhan, C.; Nie, S.; Tian, D.; Lu, J.; Wen, M.; Qiao, J.; Zhu, H.; Caiyin, Q. Enzyme and Metabolic Engineering Strategies for Biosynthesis of α-Farnesene in Saccharomyces Cerevisiae. *J. Agric. Food Chem.* **2023**, *71*, 12452–12461. [CrossRef]
20. Zhou, P.; Du, Y.; Fang, X.; Xu, N.; Yue, C.; Ye, L. Combinatorial Modulation of Linalool Synthase and Farnesyl Diphosphate Synthase for Linalool Overproduction in Saccharomyces Cerevisiae. *J. Agric. Food Chem.* **2021**, *69*, 1003–1010. [CrossRef]
21. Ojima-Kato, T.; Morishita, S.; Uchida, Y.; Nagai, S.; Kojima, T.; Nakano, H. Rapid Generation of Monoclonal Antibodies from Single B Cells by Ecobody Technology. *Antibodies* **2018**, *7*, 38. [CrossRef]
22. Goutelle, S.; Maurin, M.; Rougier, F.; Barbaut, X.; Bourguignon, L.; Ducher, M.; Maire, P. The Hill Equation: A Review of Its Capabilities in Pharmacological Modelling. *Fundam. Clin. Pharmacol.* **2008**, *22*, 633–648. [CrossRef]
23. Hernández-García, M.E.; Velázquez-Castro, J. Relationship between Decimal Hill Coefficient, Intermediate Processes, and Mesoscopic Fluctuations in Gene Expression. *ACS Omega* **2025**, *10*, 13906–13914. [CrossRef] [PubMed]
24. Hill, A.V. The Possible Effects of the Aggregation of the Molecules of Haemoglobin on Its Oxygen Dissociation Curve. *J. Physiol.* **1910**, *40*, 4–7.
25. Weiss, J.N. The Hill Equation Revisited: Uses and Misuses. *FASEB J.* **1997**, *11*, 835–841. [CrossRef] [PubMed]
26. Abeliovich, H. An Empirical Extremum Principle for the Hill Coefficient in Ligand-Protein Interactions Showing Negative Cooperativity. *Biophys. J.* **2005**, *89*, 76–79. [CrossRef]
27. Šibalić, D.; Šalić, A.; Zelić, B.; Tran, N.N.; Hessel, V.; Tišma, M. A New Spectrophotometric Assay for Measuring the Hydrolytic Activity of Lipase from Thermomyces Lanuginosus: A Kinetic Modeling. *ACS Sustain. Chem. Eng.* **2020**, *8*, 4818–4826. [CrossRef]
28. Poitevin, F.; Kushner, A.; Li, X.; Dao Duc, K. Structural Heterogeneities of the Ribosome: New Frontiers and Opportunities for Cryo-EM. *Molecules* **2020**, *25*, 4262. [CrossRef]
29. Gersteuer, F.; Morici, M.; Gabrielli, S.; Fujiwara, K.; Safdari, H.A.; Paternoga, H.; Bock, L.V.; Chiba, S.; Wilson, D.N. The SecM Arrest Peptide Traps a Pre-Peptide Bond Formation State of the Ribosome. *Nat. Commun.* **2024**, *15*, 2431, Correction in *Nat. Commun.* **2024**, *15*, 3276. [CrossRef]
30. Sato, K.; Hamada, M.; Asai, K.; Mituyama, T. CentroidFold: A Web Server for RNA Secondary Structure Prediction. *Nucleic Acids Res.* **2009**, *37*, W277–W280. [CrossRef]
31. Zur, H.; Tuller, T. Strong Association between MRNA Folding Strength and Protein Abundance in *S. cerevisiae*. *EMBO Rep.* **2012**, *13*, 272–277. [CrossRef] [PubMed]
32. Bao, C.; Zhu, M.; Nykonchuk, I.; Wakabayashi, H.; Mathews, D.H.; Ermolenko, D.N. Specific Length and Structure Rather than High Thermodynamic Stability Enable Regulatory MRNA Stem-Loops to Pause Translation. *Nat. Commun.* **2022**, *13*, 988. [CrossRef] [PubMed]
33. Fuse-Murakami, T.; Matsumoto, R.; Kanamori, T. N-Terminal Amino Acid Affects the Translation Efficiency at Lower Temperatures in a Reconstituted Protein Synthesis System. *Int. J. Mol. Sci.* **2024**, *25*, 5264. [CrossRef] [PubMed]
34. Moreira, M.H.; Barros, G.C.; Requião, R.D.; Rossetto, S.; Domitrovic, T.; Palhano, F.L. From Reporters to Endogenous Genes: The Impact of the First Five Codons on Translation Efficiency in Escherichia Coli. *RNA Biol.* **2019**, *16*, 1806–1816. [CrossRef]
35. Speicher, K.D.; Gorman, N.; Speicher, D.W. N-Terminal Sequence Analysis of Proteins and Peptides. *Curr. Protoc. Protein Sci.* **2009**, *57*, 11.10.1–11.10.31. [CrossRef]
36. Cottrell, J.S. Protein Identification Using MS/MS Data. *J. Proteomics* **2011**, *74*, 1842–1851. [CrossRef]

37. Cook, S.A. Understanding Interleukin 11 as a Disease Gene and Therapeutic Target. *Biochem. J.* **2023**, *148*, 1987–2008. [CrossRef]
38. Giguère, P.M.; Gall, B.J.; Ezekwe, E.A.D.; Laroche, G.; Buckley, B.K.; Kebaier, C.; Wilson, J.E.; Ting, J.P.; Siderovski, D.P.; Duncan, J.A. G Protein Signaling Modulator-3 Inhibits the Inflammasome Activity of NLRP3. *J. Biol. Chem.* **2014**, *289*, 33245–33257. [CrossRef]
39. Nezametdinova, V.Z.; Yunes, R.A.; Dukhinova, M.S.; Alekseeva, M.G.; Danilenko, V.N. The Role of the PFNA Operon of Bifidobacteria in the Recognition of Host's Immune Signals: Prospects for the Use of the FN3 Protein in the Treatment of COVID-19. *Int. J. Mol. Sci.* **2021**, *22*, 9219. [CrossRef]

Disclaimer/Publisher's Note: The statements, opinions and data contained in all publications are solely those of the individual author(s) and contributor(s) and not of MDPI and/or the editor(s). MDPI and/or the editor(s) disclaim responsibility for any injury to people or property resulting from any ideas, methods, instructions or products referred to in the content.